European Conference on Computational Mechanics
Solids, Structures and Coupled Problems in Engineering
C.A. Mota Soares et.al. (eds.)
Lisbon, Portugal, 5–8 June 2006

3D HOMOGENIZED LIMIT ANALYSIS OF MASONRY BUILDINGS SUBJECTED TO HORIZONTAL LOADS

G.Milani[1], P.B.Lourenço[2], A. Tralli[1]

[1] Department of Engineering, University of Ferrara
Via Saragat 1 44100 Ferrara, Italy
gmilani@ing.unife.it
atralli@ing.unife.it

[2] Department of Civil Engineering, University of Minho, School of Engineering
4800-058 Azurem, Guimarães, Portugal
pbl@civil.uminho.pt

Keywords: Masonry, limit analysis, kinematic approach, 3D.

Abstract. *The current confidence in the ability to provide buildings with adequate resistance to horizontal actions does not extend back to historic and existing masonry structures. Furthermore, it has been shown that the high vulnerability of historical centers to horizontal actions is mostly due to the absence of adequate connections between the various parts, especially when wooden beams are present both in the floors and in the roof [1]. This characteristic leads to overturning collapses of the perimeter walls under seismic horizontal acceleration and combined in- and out-of-plane failures. Even if limit analysis is not sufficient for a full structural analysis under seismic loads, it can be profitably used in order to obtain a simple and quick estimation of collapse loads and failure mechanisms. Up to now, simplified limit analysis methods are at disposal to the practitioners both for safety analyses and design of strengthening [2]. Nevertheless, in some cases these methods are based on several simplifications, one of which is an a-priori assumption of the collapse mechanics combined with the separation of in- and out-of-plane effects. In this paper, the micro-mechanical model presented by the authors in [3] and [4] for the limit analysis of respectively in- and out-of-plane loaded masonry walls is utilized in presence of coupled membrane and flexural effects. In the model, the elementary cell is subdivided along its thickness in several layers. For each layer, fully equilibrated stress fields are assumed, adopting polynomial expressions for the stress tensor components in a finite number of sub-domains. The continuity of the stress vector on the interfaces between adjacent sub-domains and suitable anti-periodicity conditions on the boundary surface are further imposed. In this way, linearized homogenized surfaces in six dimensions (polytopes) for masonry in- and out-of-plane loaded are obtained. Such surfaces are then implemented in a FE limit analysis code for the analysis at collapse of entire 3D structures. Two examples of technical relevance are discussed in detail and comparisons with results obtained by means of standard FE codes are provided.*

1 INTRODUCTION

The evaluation of the ultimate load bearing capacity of entire masonry buildings subjected to horizontal loads is a fundamental task for the design of brickwork structures. Furthermore, many codes of practice, as for instance the recent Italian O.P.C.M. 3431 [5] [6], require a static non linear analysis for existing masonry buildings, in which a limited ductile behavior of the elements is taken into account, featuring failures connected to rocking, shear and diagonal cracking of the walls.

Nowadays, several models for the analysis of masonry buildings are at disposal, but the approach based on the use of averaged constitutive equations seems to be the only one suitable to be employed in a large scale finite element analysis [7]. In fact, a heterogeneous approaches based on a distinct representation of bricks and joints seems to be limited to the study of panels of small dimensions, due to the large number of variables involved in a non linear finite element analysis. Therefore, alternative strategies based on macro-modeling have been recently developed in order to tackle engineering problems. Nevertheless, macro-approaches require a preliminary mechanical characterization of the model, which has to be derived from experimental data [8].

In this framework, homogenization techniques can be profitably used for the analysis of large scale structures. In this case, in fact, both mechanical properties of constituent materials and geometry of the elementary cell are taken into account only at a cell level, so allowing the analysis of entire buildings through standard finite element codes. Furthermore, the application of homogenization theory to the rigid-plastic case [9] requires only a reduced number of material parameters and provides important information at failure, such as limit multipliers, collapse mechanisms and, at least on critical sections, the stress distribution [10].

In this paper, the micro-mechanical model presented by the authors in [3] and [4] for the limit analysis of respectively in- and out-of-plane loaded masonry walls is utilized in presence of coupled membrane and flexural effects. In the model, the elementary cell is subdivided along its thickness in several layers. For each layer, fully equilibrated stress fields are assumed, adopting polynomial expressions for the stress tensor components in a finite number of sub-domains. The continuity of the stress vector on the interfaces between adjacent sub-domains and suitable anti-periodicity conditions on the boundary surface are further imposed. In this way, linearized homogenized surfaces in six dimensions (polytopes) for masonry in- and out-of-plane loaded are obtained. Such surfaces are then implemented in a FE limit analysis code for the analysis at collapse of entire 3D structures. Two examples of technical relevance are discussed in detail and comparisons with standard FE codes are provided.

In Section 2, the micro-mechanical model adopted for obtaining masonry homogenized polytopes is recalled, whereas in Section 3 the FE upper bound approach is presented. The method is based on a triangular discretization of the structure, so that the velocity field interpolation is linear inside each element. Plastic dissipation can occur for in-plane actions both in continuum and in interfaces, whereas out-of-plane dissipation takes place only at the interface between adjacent triangles. Two meaningful structural examples are treated in detail in Section 4, concerning a large scale masonry building located in Ferrara (Italy) and an ancient house already studied by De Benedictis et al. in [11]. The reliability of the proposed model is assessed through comparisons with results obtained by means of standard non-linear FE approaches.

2 IN- AND OUT-OF-PLANE HOMOGENIZED FAILURE SURFACES

A masonry wall Ω constituted by a periodic arrangement of bricks and mortar disposed in running bond texture is considered, as shown in Figure 1-a. As pointed out by Suquet in [9],

homogenization techniques combined with limit analysis can be applied for the evaluation of the homogenized out-of-plane strength domain S^{hom} of masonry. Under the assumptions of perfect plasticity and associated flow rule for the constituent materials, and in the framework of the lower bound limit analysis theorem, S^{hom} can be derived by means of the following (non-linear) optimization problem (see also Figure 1):

$$S^{\text{hom}} = \left\{ (\mathbf{M},\mathbf{N}) \,|\, \left\{ \begin{array}{rl} \mathbf{N} = \dfrac{1}{|Y|}\displaystyle\int_{Y\times h} \boldsymbol{\sigma} dV & (a) \\ \mathbf{M} = \dfrac{1}{|Y|}\displaystyle\int_{Y\times h} y_3 \boldsymbol{\sigma} dV & (b) \\ div\boldsymbol{\sigma} = \mathbf{0} & (c) \\ [\![\boldsymbol{\sigma}]\!]\mathbf{n}^{\text{int}} = \mathbf{0} & (d) \\ \boldsymbol{\sigma}\mathbf{n} \quad \text{anti-periodic} \quad \text{on} \quad \partial Y_l & (e) \\ \boldsymbol{\sigma}(\mathbf{y}) \in S^m \quad \forall \mathbf{y} \in Y^m \;;\; \boldsymbol{\sigma}(\mathbf{y}) \in S^b \quad \forall \mathbf{y} \in Y^b & (f) \end{array} \right\} \right\} \qquad (1)$$

where:

- $\mathbf{N}$ and $\mathbf{M}$ are the macroscopic in-plane (membrane forces) and out-of-plane (bending moments and torsion) tensor;
- $\boldsymbol{\sigma}$ denotes the microscopic stress tensor;
- $\mathbf{n}$ is the outward versor of ∂Y_l surface, Figure 1-a;
- ∂Y_l is defined in Figure 1-a;
- $[\![\boldsymbol{\sigma}]\!]$ is the jump of micro-stresses across any discontinuity surface of normal $\mathbf{n}^{\text{int}}$, Figure 1-c;
- S^m and S^b denote respectively the strength domains of mortar and bricks;
- Y is the cross section of the 3D elementary cell with $y_3 = 0$ (see Figure 1) $|Y|$ is its area, V is the elementary cell, h represents the wall thickness and $\mathbf{y} = (y_1 \quad y_2 \quad y_3)$;
- condition (1-c) imposes the micro-equilibrium with zero body forces, usually neglected in the framework of the homogenization theory;
- anti-periodicity condition (1-e) requires that that stress vectors $\boldsymbol{\sigma}\mathbf{n}$ are opposite on opposite sides of ∂Y_l, Figure 1-c, i.e. $\sigma^{(m)}\mathbf{n}_1 = -\sigma^{(n)}\mathbf{n}_2$.

In order to solve (1) numerically, the simple admissible and equilibrated micro-mechanical model proposed in [4] is adopted. The unit cell is subdivided into a fixed number of layers along its thickness, as shown in Figure 1-b. For each layer out-of-plane components σ_{i3} $(i = 1, 2, 3)$ of the micro-stress tensor $\boldsymbol{\sigma}$ are set to zero, so that only in-plane components σ_{ij} $(i, j = 1, 2)$ are considered active. Furthermore, σ_{ij} $(i, j = 1, 2)$ are kept constant along the Δ_{i_L} thickness of each layer, i.e. in each layer $\sigma_{ij} = \sigma_{ij}(y_1, y_2)$. For each layer one-fourth of the REV is sub-divided into nine geometrical elementary entities (sub-domains), so that the entire cell is sub-divided into 36 sub-domains (see [4] for further details and Figure 1-b).

For each sub-domain (k) and layer (i_L), polynomial distributions of degree (m) in the variables (y_1, y_2) are a priori assumed for the stress components. Since stresses are polynomial expressions, the generic ij th component can be written as follows:

$$\sigma_{ij}^{(k,i_L)} = \mathbf{X}(\mathbf{y})\mathbf{S}_{ij}^{(k,i_L)T} \quad \mathbf{y} \in Y^{(k,i_L)} \qquad (2)$$

where:

- $\mathbf{X}(\mathbf{y}) = \lfloor 1 \quad y_1 \quad y_2 \quad y_1^2 \quad y_1 y_2 \quad y_2^2 \quad \ldots \rfloor$;
- $\mathbf{S}_{ij}^{(k,i_L)} = \lfloor S_{ij}^{(k,i_L)(1)} \quad S_{ij}^{(k,i_L)(2)} \quad S_{ij}^{(k,i_L)(3)} \quad S_{ij}^{(k,i_L)(4)} \quad S_{ij}^{(k,i_L)(5)} \quad S_{ij}^{(k,i_L)(6)} \quad \ldots \rfloor$ is a vector representing the unknown stress parameters of sub-domain (k) of layer (i_L);
- $Y^{(k,i_L)}$ represents the k th sub-domain of layer (i_L).

The imposition of equilibrium inside each sub-domain (with zero body forces, as usual in homogenization procedures), the continuity of the stress vector on interfaces and the anti-periodicity of $\boldsymbol{\sigma}\mathbf{n}$ permit a strong reduction of the number of independent stress parameters. For the sake of conciseness, we refer the reader to [3] for further details.

Elementary assemblage operations on the local variables allow to write the stress vector $\widetilde{\boldsymbol{\sigma}}^{(k,i_L)}$ of layer i_L inside each sub-domain as:

$$\widetilde{\boldsymbol{\sigma}}^{(k,i_L)} = \widetilde{\mathbf{X}}^{(k,i_L)}(\mathbf{y})\widetilde{\mathbf{S}}^{(i_L)} \quad k = 1,\ldots, \text{ num. } sub-domains\, i_L = 1,\ldots,\text{num. } layers \tag{3}$$

where $\widetilde{\mathbf{S}}^{(i_L)}$ is the vector of unknown stress parameters of layer i_L.

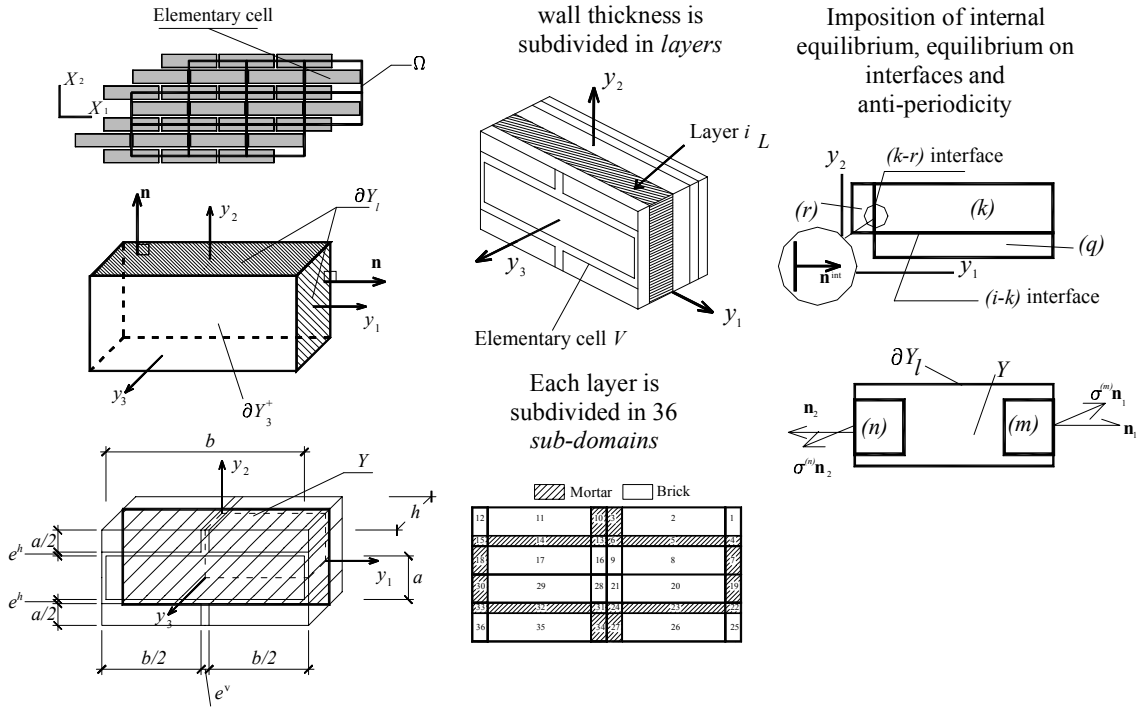

Figure 1: The micro-mechanical model proposed. -a: the elementary cell. –b: subdivision in layers along the thickness and subdivision of each layer in sub-domains. –c: imposition of internal equilibrium, equilibrium on interfaces and anti-periodicity.

As already pointed out, once that an equilibrated polynomial field in each layer is obtained, the proposed out-of-plane model requires a subdivision (n_L) of the wall thickness into several layers (Figure 1-a), with a fixed constant thickness $\Delta_{i_L} = t / n_L$ for each layer. This allows to derive the following simple (non) linear optimization problem:

$$S^{\hom} \equiv \left\{ \begin{array}{l} \max\{\lambda\} \\ such\ that \left\{ \begin{array}{ll} \widetilde{\mathbf{N}} = \int\limits_{k,i_L} \widetilde{\boldsymbol{\sigma}}^{(k,i_L)} dV & (a) \\ \widetilde{\mathbf{M}} = \int\limits_{k,i_L} y_3 \widetilde{\boldsymbol{\sigma}}^{(k,i_L)} dV & (b) \\ \boldsymbol{\Sigma} = \left[\widetilde{\mathbf{N}} \quad \widetilde{\mathbf{M}}\right] = \lambda \mathbf{n}_{\Sigma} & (c) \\ \widetilde{\boldsymbol{\sigma}}^{(k,i_L)} = \widetilde{\mathbf{X}}^{(k,i_L)}(\mathbf{y})\widetilde{\mathbf{S}} & (d) \\ \widetilde{\boldsymbol{\sigma}}^{(k,i_L)} \in S^{(k,i_L)} & (e) \\ k = 1,\ldots, \text{ number of } sub-domains & (f) \\ i_L = 1,\ldots, \text{number of } layers & (g) \end{array} \right. \end{array} \right. \qquad (4)$$

where:

- λ is the load multiplier (ultimate moment, ultimate membrane action or a combination of moments and membrane actions) with fixed direction $\mathbf{n}_{\Sigma}$ in the six dimensional space of membrane actions ($\widetilde{\mathbf{N}} = \left[N_{xx} \ N_{xy} \ N_{yy}\right]$) and bending torsion moments ($\widetilde{\mathbf{M}} = \left[M_{xx} \ M_{xy} \ M_{yy}\right]$).
- $S^{(k,i_L)}$ denotes the (non-linear) strength domain of the constituent material (mortar or brick) corresponding to the k^{th} sub-domain and i_L^{th} layer.
- $\widetilde{\mathbf{S}}$ collects all the unknown polynomial coefficients (of each sub-domain of each layer).

In what follows, wall thickness is subdivided into at least thirty layers. Authors experienced that more refined discretizations do not allow technically meaningful improvements in the accuracy of the homogenized failure surface.

It is worth noting that the model at hand is able to reproduce the typical anisotropic behavior of masonry at failure, as well as a zero tensile strength if a Mohr-Coulomb failure criterion with cohesion equal to zero is assumed for joints.

3 3D KINEMATIC FE LIMIT ANALYSIS: BASIC ASSUMPTIONS

The upper bound approach developed in this paper is based both on the formulation presented in [12] by Sloan and Kleeman for the in-plane case and on the formulation by Munro and Da Fonseca [13] [14] for out-of-plane actions.

Both formulations use three noded triangular elements with linear interpolation of the velocity field inside each element. In addition, for the in-plane case discontinuities of the velocity field along the edges of adjacent triangles are introduced. It has been shown [3] [12], in fact, that the definition of kinematically admissible velocity fields with discontinuities on interfaces is adequate for purely cohesive or cohesive-frictional materials, which is the case of masonry.

For each element E, three velocity unknowns per node i, say w_{xx}^i , w_{yy}^i and w_{zz}^i (respectively 2 in-plane velocities and 1 out-of-plane velocity, see Figure 2-a) are introduced, so that the velocity field is linear inside an element, whereas the strain rate field is constant for in-plane actions.

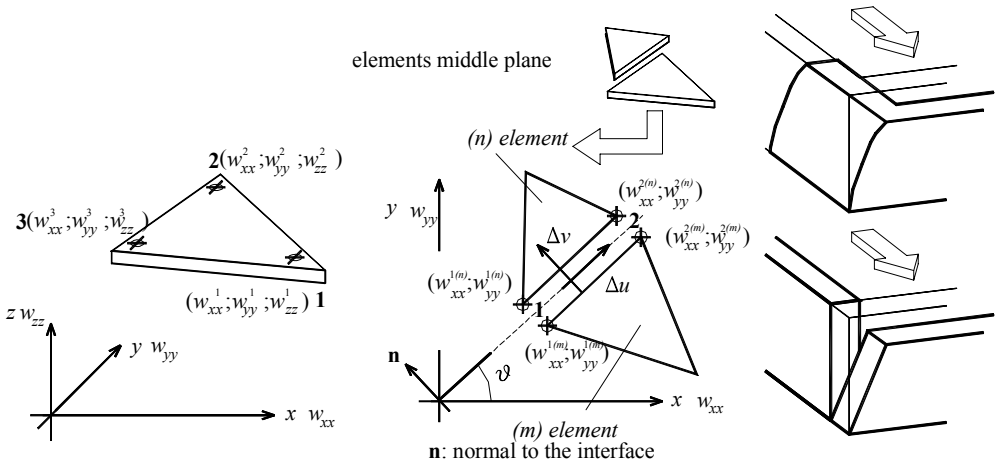

-a -b -c

Figure 2: -a: Triangular plate and shell element used for the upper bound FE limit analysis. –b: discontinuity of the in-plane velocity field. –c: perfect interlocking and absence of connections between perpendicular walls.

For the sake of simplicity, it is assumed that jump of velocities on interfaces occurs only in the plane containing two contiguous and coplanar elements, with linear interpolation of the jump along the interface. Hence, for each interface between coplanar adjacent elements, four adding unknowns are introduced ($\Delta\mathbf{u}^I = [\Delta v_1\ \Delta u_1\ \Delta v_2\ \Delta u_2]^T$), representing the normal (Δv_i) and tangential (Δu_i) jumps of velocities (with respect to the discontinuity direction) evaluated on nodes $i=1$ and $i=2$ of the interface (see Figure 2-b). For the sake of simplicity, it is assumed in the model that, if two adjacent elements do not lay in the same plane, no discontinuity occur between the velocities belonging to the elements, so a priori assuming a perfect interlocking between perpendicular walls (see Figure 2-c).

Hence, for any pair of nodes on the interface between two adjacent and coplanar triangles $(m)-(n)$, the tangential and normal velocity jumps can be written in terms of the Cartesian nodal velocities of elements $(m)-(n)$ (see [12] for details), so that four linear equations in the following form can be written:

$$\mathbf{A}_{11}^{eq}\mathbf{w}^{Em} + \mathbf{A}_{12}^{eq}\mathbf{w}^{En} + \mathbf{A}_{13}^{eq}\Delta\mathbf{u}^I = \mathbf{0} \qquad (5)$$

where $\mathbf{w}^{Em}$ and $\mathbf{w}^{En}$ are the $9x1$ vectors that collect velocities of elements (m) and (n) respectively.

For continuum under in-plane loads three equality constrains representing the plastic flow in continuum (obeying an associated flow rule) are introduced for each element:

$$\dot{\boldsymbol{\varepsilon}}_{pl}^{E} = \left[\frac{\partial u_{xx}}{\partial x}\quad \frac{\partial u_{yy}}{\partial y}\quad \frac{\partial u_{yy}}{\partial x}+\frac{\partial u_{xx}}{\partial y}\right] = \dot{\lambda}^{E}\frac{\partial S^{\hom}}{\partial \boldsymbol{\Sigma}} \qquad (6)$$

Where:

- $\dot{\boldsymbol{\varepsilon}}_{pl}^{E}$ is the plastic strain rate vector of element E;
- $\dot{\lambda}^{E} \geq 0$ is the plastic multiplier;
- $S^{\hom}$ is the homogenized (non) linear failure polytope of masonry.

It is worth noting that out-of-plane components of the plastic strain rate are $\dot{\gamma}_{pl,xz} = \dot{\gamma}_{pl,yz} = 0$ whereas $\dot{\varepsilon}_{pl,zz}$ is constant.

We refer the reader to the previous section and to [4] for further details on the procedure used for obtaining a linear approximation (with m hyper-planes) of the failure polytope in the form $S^{\hom} \equiv \mathbf{A}^{in}\boldsymbol{\Sigma} \le \mathbf{b}^{in}$.

Three linear equality constraints per element can be written in the form $\mathbf{A}_{11}^{eq}\mathbf{w}^{E} + \mathbf{A}_{12}^{eq}\dot{\boldsymbol{\lambda}}^{E} = \mathbf{0}$, where $\mathbf{w}^{E}$ is the vector of element velocities and $\dot{\boldsymbol{\lambda}}^{E}$ is a $mx1$ vector of plastic multiplier rates (one for each plane of the linearised failure surface).

Following Munro and Da Fonseca [13], out-of-plane plastic dissipation occurs only along each interface I between two adjacent triangles R and K or on a boundary side B of an element Q (see Figure 3).

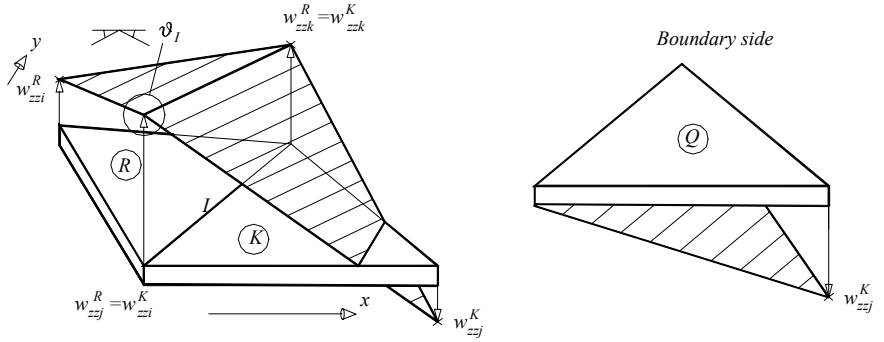

Figure 3: Rotation along an interface between adjacent triangles or in correspondence of a boundary side.

Denoting with $\mathbf{w}_{zz,E} = \begin{bmatrix} w_{zz,i}^{E} & w_{zz,j}^{E} & w_{zz,k}^{E} \end{bmatrix}^{T}$ element E out-of-plane nodal velocities and with $\boldsymbol{\theta}_{E} = \begin{bmatrix} \vartheta_{i}^{E} & \vartheta_{j}^{E} & \vartheta_{k}^{E} \end{bmatrix}^{T}$ side normal rotations, $\boldsymbol{\theta}_{E}$ and $\mathbf{w}_{zz,E}$ are linked by the compatibility equation (Figure 3):

$$\boldsymbol{\theta}_{E} = \mathbf{B}_{E}\mathbf{w}_{zz,E} \qquad (7)$$

- where $\mathbf{B}_{E} = \dfrac{1}{2A_{E}}\begin{bmatrix} \dfrac{b_i b_i + c_i c_i}{l_i} & \dfrac{b_i b_j + c_i c_j}{l_i} & \dfrac{b_i b_k + c_i c_k}{l_i} \\ \dfrac{b_j b_i + c_j c_i}{l_j} & \dfrac{b_j b_j + c_j c_j}{l_j} & \dfrac{b_j b_k + c_j c_k}{l_j} \\ \dfrac{b_k b_i + c_k c_i}{l_k} & \dfrac{b_k b_j + c_k c_j}{l_k} & \dfrac{b_k b_k + c_k c_k}{l_k} \end{bmatrix}$, with $b_i = y_j - y_k$, $c_i = x_k - x_j$

ad A_E element area.

Total internal power dissipated P^{in} is constituted by power dissipated in continuum P_E^{in} and power dissipated on interfaces P_I^{in}.

P_E^{in} can be evaluated for each triangle E of area A taking into account that curvature rates $\dot{\chi}_{xx}$, $\dot{\chi}_{xy}$, $\dot{\chi}_{yy}$ are zero in continuum, so that flexural part does not dissipate in continuum. Hence, supposing (as already pointed out) the homogenized (linearised) failure surface constituted by m planes of equation $A_{xx}^{q}N_{xx} + A_{yy}^{q}N_{yy} + A_{xy}^{q}N_{xy} + B_{xx}^{q}M_{xx} + B_{yy}^{q}M_{yy} +$

$+B_{xy}^{q}M_{xy}=C_{E}^{q}\quad 1\le q\le m$ a projection of $S^{\hom}$ in the space $M_{xx}=M_{yy}=M_{xy}=0$ can be used in order to have an estimation of P_E^{in}:

$$P_E^{in}=A\sum_{q=1}^{m}C_E^q\dot{\lambda}_E^{(q)} \tag{8}$$

where $\dot{\lambda}_E^{(q)}$ is the plastic multiplier rate of the triangle E associated to the q th hyper-plane of the linearised failure surface.

Power dissipated P_I^{in} along an interface I of length Γ can be written as follows:

$$\begin{aligned}
&P_I^{in}=P_{I-M}^{in}+P_{I-N}^{in}=\Gamma M_{nn,I}^{+}\vartheta_I+\Gamma/2\sum_{q=1}^{m^I}C_I^q\left(\dot{\lambda}_{Ii}^{(q)}+\dot{\lambda}_{If}^{(q)}\right)\quad \vartheta_I>0\\
&P_I^{in}=P_{I-M}^{in}+P_{I-N}^{in}=\Gamma M_{nn,I}^{-}\left|\vartheta_I\right|+\Gamma/2\sum_{q=1}^{m^I}C_I^q\left(\dot{\lambda}_{Ii}^{(q)}+\dot{\lambda}_{If}^{(q)}\right)\quad \vartheta_I<0
\end{aligned} \tag{9}$$

Where:

- $\vartheta_I=\vartheta_i^R+\vartheta_j^K$ is the relative rotation between R and K along I (see Figure 3);
- $\dot{\lambda}_{Ii}^{(q)}$ and $\dot{\lambda}_{If}^{(q)}$ represent respectively the q th plastic multiplier rate of the initial (i) and final (f) point of the interface I, being the variation of plastic multiplier rates on interfaces linear. For the interfaces, a projection of the failure surfaces is required, which depends on the orientation ϑ of the interface with respect to the horizontal direction;
- $M_{nn,I}^{+}$ and $M_{nn,I}^{-}$ are positive and negative failure bending moments along I. An approach for obtaining an upper bound estimation of $M_{nn,I}^{+}$ and $M_{nn,I}^{-}$ from the actual strength domain ($S^{\hom}$) of the homogenized material can be found in [4] and we refer the reader there for further details. A similar expression can be obtained considering a boundary side B of an element Q, Figure 3.

Since the internal power dissipated on interfaces (9) is non-linear, positive and negative rotations are introduced as follows: $P_{I-M}^{in}=\Gamma\left(M_{nn,I}^{+}\vartheta_I^{+}+M_{nn,I}^{-}\vartheta_I^{-}\right)\quad \vartheta_I=\vartheta_I^{+}-\vartheta_I^{-}\quad \vartheta_I^{+};\vartheta_I^{-}\ge 0$.

External power dissipated can be written as $P^{ex}=\left(\mathbf{P}_0^T+\lambda\mathbf{P}_1^T\right)\mathbf{w}$, where $\mathbf{P}_0$ is the vector of (equivalent lumped) permanent loads, λ is the load multiplier, $\mathbf{P}_1^T$ is the vector of (lumped) variable loads and $\mathbf{w}$ is the vector of assembled nodal velocities. As the amplitude of the failure mechanism is arbitrary, a further normalization condition $\mathbf{P}_1^T\mathbf{w}=1$ is usually introduced. Hence, the external power becomes linear in $\mathbf{w}$ and λ, i.e. $P^{ex}=\mathbf{P}_0^T\mathbf{w}+\lambda$.

After some elementary assemblage operations, a simple linear programming problem is obtained (analogous to that reported in [12]), where the objective function consists in the minimization of the total internal power dissipated:

$$\begin{cases}\min\left\{\sum_{I=1}^{n^I}P_I^{in}+\sum_{E=1}^{n^E}P_E^{in}-\mathbf{P}_0^T\mathbf{w}\right\}\\ \text{such that}\begin{cases}\mathbf{A}^{eq}\mathbf{U}=\mathbf{b}^{eq}\\ \dot{\boldsymbol{\lambda}}^{I,ass}\ge\mathbf{0}\quad\dot{\boldsymbol{\lambda}}^{E,ass}\ge\mathbf{0}\\ \boldsymbol{\theta}^{+}\ge 0\quad\boldsymbol{\theta}^{-}\ge 0\end{cases}\end{cases} \tag{10}$$

where:

- $\mathbf{U}$ is the vector of global unknowns and collects the vector of assembled nodal velocities ($\mathbf{w}$), the vector of assembled element plastic multiplier rates ($\dot{\boldsymbol{\lambda}}^{E,ass}$), the vector of assembled jump of velocities on interfaces ($\Delta\mathbf{u}^{I,ass}$), the vector of assembled interface plastic multiplier rates ($\dot{\boldsymbol{\lambda}}^{I,ass}$) and $\boldsymbol{\theta}^{+}$ and $\boldsymbol{\theta}^{-}$ vectors, positive and negative interface and boundary rotation angles.
- $\mathbf{A}^{eq}$ is the overall constraints matrix and collects normalization condition, velocity boundary conditions, relations between velocity jumps on interfaces and elements velocities, constraints for plastic flow in velocity discontinuities and constraints for plastic flow in continuum.
- n^{E} and n^{I} are the total number of elements and interfaces, respectively.

We refer the reader to [15] and [16] for a critical discussion of the most efficient tools for solving problem (10).

4 STRUCTURAL EXAMPLES

In this section, two structural examples are presented, namely a three storey masonry building located in Ferrara (Italy) and a two storey house, already studied both by De Benedictis et al. in [11] and by Orduna in [17]. In both cases a homogenized limit analysis approach is used to predict the ultimate shear at the base for seismic actions. In both analyses, the so called primary collapse mechanisms, as for instance the overturning of a single façade, are excluded imposing perfect interlocking at each corner.

In this manner, the limit analysis approach proposed can be compared with standard FE elastic-plastic analyses performed by means of commercial codes (Strand 7.2). Both failure mechanisms and failure loads show that technically meaningful results can be obtained with the model at hand.

It is worth noting that the usefulness of a global limit analysis conducted by means of plate and shell elements on entire buildings stands in its capability to take into account simultaneously in- and out-of-plane failures, as well as partial collapse mechanism of single panels. Furthermore, an a-priori estimation of the most probable collapse mechanism is not required.

4.1 3D Limit Analysis of Alfonso Varano School, Ferrara, Italy

The example treated here consists in the prediction of the failure horizontal load of a three storey masonry building located in Ferrara (Italy), see Figure 4. The analysis has been conducted within a research project carried on at the University of Ferrara in cooperation with the "Amministrazione Provinciale di Ferrara", with the aim of assessing the seismic vulnerability of the school buildings belonging to "Provincia di Ferrara". The building, erected at the end of 19th century, is a school standing in Via Ghiara, Ferrara, in an isolated position and consists in two structurally independent rectangular main bodies, as shown in the plan view reported in Figure 5.

The main building, called here for the sake of simplicity "Body A" presents a rectangular shape with dimensions L_1xL_2=49,05x12,20 m and 3 storeys, whereas the secondary "Body B" has a rectangular shape L_1xL_2= 8x13 m and 3 storeys. All the walls are realized with artificial clay bricks, assumed of dimensions 250x120x55 mm^3 in absence of precise information. First storey height is 485 cm whereas second and third storeys height is 465 cm.

In a restoration intervention executed during the 1980's decade a 2 cm separation joint was introduced between body A and B. Therefore, only body A is here taken into consideration for the sake of simplicity.

"Body A" is geometrically regular with equally distributed mass, except for the large openings at the center of the first floor of the three walls parallel to x direction, which are part of a corridor giving the access to the building. A main corridor of access to classrooms is located between walls x-1 and x-2, Figure 5. Walls thickness is reported in Table I.

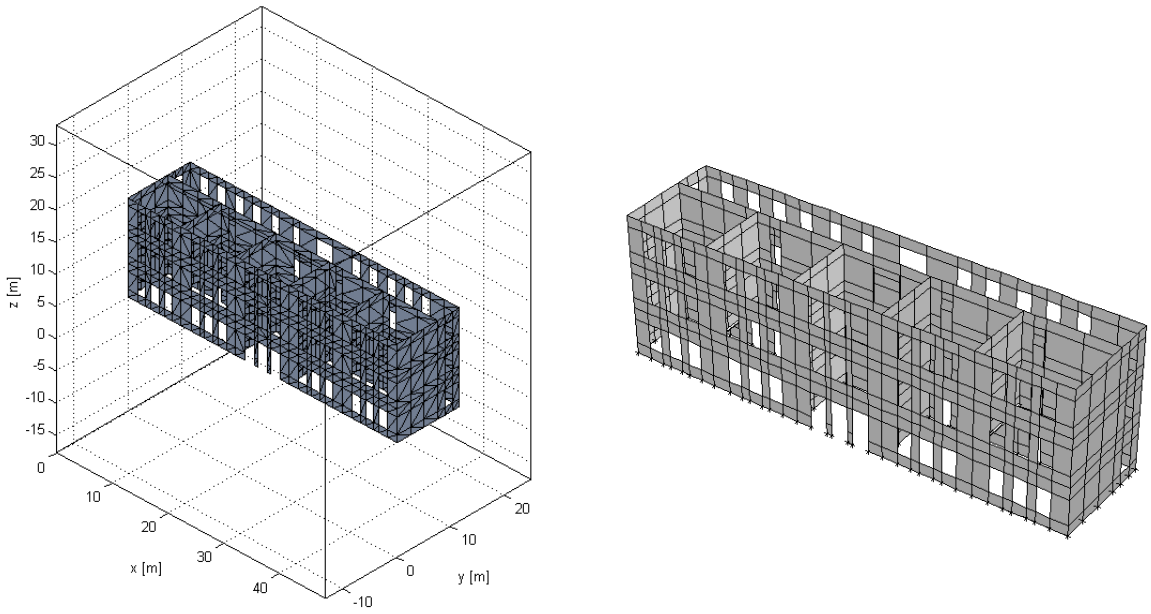

-a -b

Figure 4: -a: Mesh used for the limit analysis (1576 triangular elements) and (-b) mesh used in Strand 7.2 for an elastic-plastic analysis with Mohr-Coulomb failure criterion.

Table I: Walls thickness (cm), Alfonso Varano building.

storey	x-1	x-2	x-3	y-1	y-2	y-3
1	60	45	60	60	45	-
2	50	45	50	50	45	45
3	45	30	45	45	30	30

A FE model consisting of 1576 triangular elements is used for performing the homogenized limit analysis proposed (Figure 4-a) under a static equivalent seismic load directed along x-direction direction. The results obtained with the homogenized FE limit analysis model (i.e. failure shear at the base and failure mechanism) are compared with a standard FE elastic-perfectly plastic analysis conducted by means of a standard FE model. The analysis is performed using a mesh of 788 four noded shell elements supposing masonry isotropic with a pure Mohr-Coulomb failure criterion.

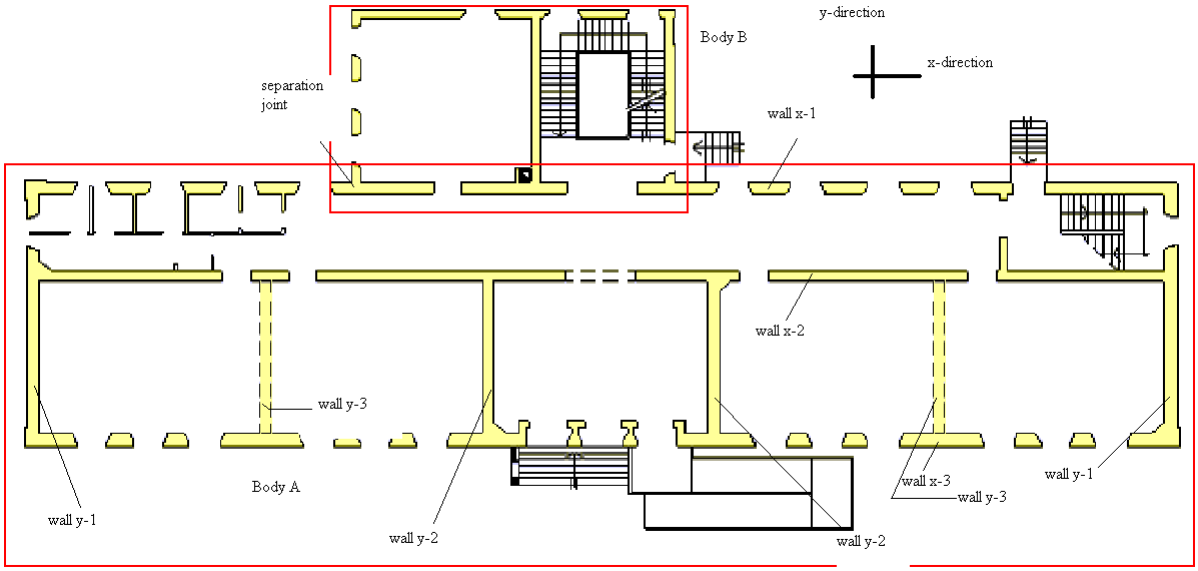

Figure 5: First floor plan view, Alfonso Varano school.

For masonry, a cohesion c equal to $\hat{c} = 0.12 \frac{N}{mm^2}$ and friction angle $\phi = \hat{\phi} = \tan^{-1}(0.4)$ are adopted for the simulations, in agreement with the Italian code [5] [6]. In order to compare the homogenized limit analysis procedure proposed with the standard FE model, a linearized Lourenço-Rots [18] [19] failure criterion for joints is adopted for the homogenization approach, whereas for units a linear cut-off failure criterion in compression is assumed, see Table II.

Table II: Mechanical characteristics assumed for joints and bricks.

Joint					*Unit*
$c\ [N/mm^2]$	$f_t\ [N/mm^2]$	$f_c\ [N/mm^2]$	Φ_1	Φ_2	$f_c\ [N/mm^2]$
0.12	0.12	15	$\tan^{-1}(0.4)$	90°	30

In both models, the seismic load is applied in correspondence of floor i by means of a horizontal distributed load of intensity $k_i \hat{\lambda}$ (k_i constant), where $\hat{\lambda}$ is the limit multiplier and k_i is taken, in agreement with the Italian code [5], equal to $z_i W_i / \left(\sum_i^n z_i W_i \right)$, where W_i is the ith floor vertical load, z_i is the ith floor altitude and n is the total number of floors.

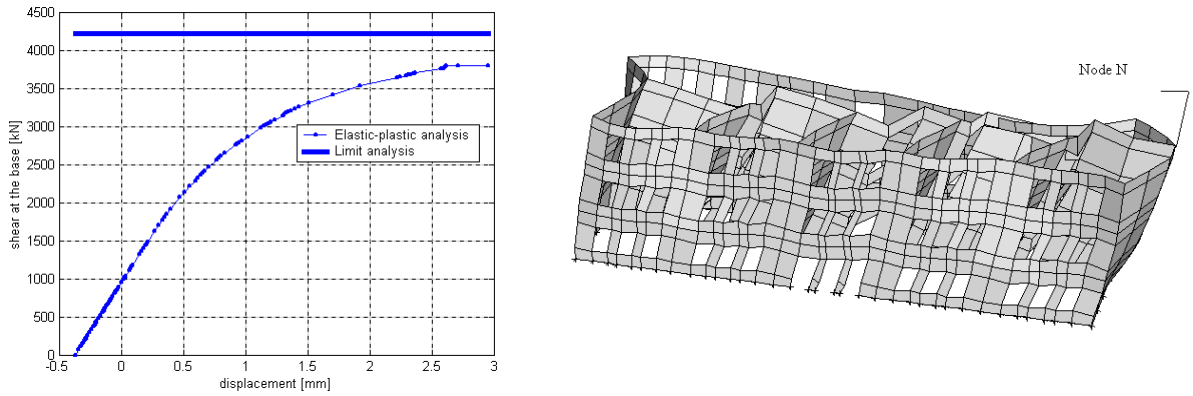

Figure 6: Standard FE elastic plastic approach. –a: shear at the base - node N displacement curve. -b: deformed shape at collapse.

Floors, constituted by small vaults made of clay bricks and supported by a framework of steel girders, are disposed parallel to y-direction in correspondence of first and second floors and distribute vertical loads uniformly on x-directed walls. As a first attempt, floors stiffness is not taken into account in the numerical model and vertical loads, which are independent from the load multiplier, are applied directly on masonry walls in correspondence of the floors. In correspondence of the third floor, a timber truss structure supports an inclined roof covering. For the sake of simplicity, self weight of masonry is supposed concentrated in correspondence of the floors and added to the remaining dead loads, which are defined according to the Italian code [20] (see also [21] and [22]).

The kinematic FE homogenized limit analysis gives a total shear at the base of the building of $4220\,kN$, in good agreement with the results obtained with the standard FE procedure. In this latter case, in fact, the capacity curve of the building, Figure 6-a, reaches its maximum at approximately $3800\,kN$. Finally, the deformed shape at collapse of both models, Figure 6-b and Figure 7, demonstrates that a combined in- and out-of-plane failure takes place and that failure is mainly concentrated along walls x-2 and x-3.

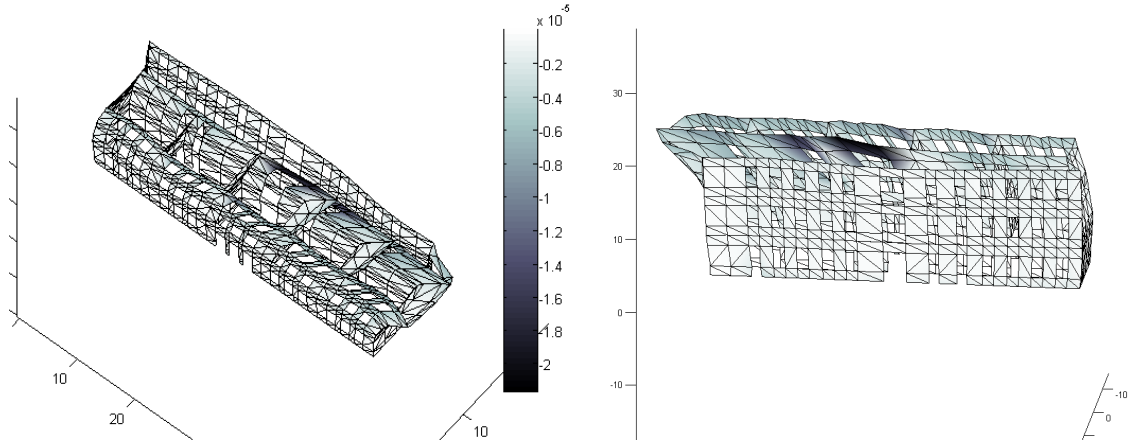

Figure 7: Deformed shape at collapse and concentration of plastic dissipation for the entire building, homogenization FE limit analysis approach.

4.2 3D Limit Analysis of an ancient masonry building

In this section, a 3D FE limit analysis on an ancient masonry building is presented. The model is an adaptation of a real house analyzed by De Benedictis et al. in [11]. It is worth noting that the same example has been studied by Orduna in [17] by means of a macro-blocks approach and using limit analysis. The building has two storeys and it is assumed, for the sake of simplicity, that its plan is rectangular, with dimensions 8.30x5.35 m.
Vertical load is constituted by walls self weight and permanent and accidental loads of the first floor and of the roof.

Masonry density is assumed equal to $20\,kN/m^2$. Due to the elevate thickness of the walls, masonry self weight represents a not negligible percentage of the total vertical load.
First floor permanent and accidental loads are assumed respectively equal to $1.61\,kN/m^2$ and $2\,kN/m^2$. On the other hand, roof permanent and accidental loads are assumed respectively equal to $0.87\,kN/m^2$ and $1\,kN/m^2$.When seismic load acts, accidental loads are reduced by means of a coefficient equal to $1/3$.

In Figure 8, a three dimensional representation of the model is reported. Walls AB and DC are assumed 60 cm thick at the first storey and 45 cm at the second storey, whereas walls AD and BC are 74 cm and 52 cm thick respectively. Wall AD is shared with a contiguous building, consequently only a positive seismic action along X direction is taken into account.

As underlined by De Benedictis et al. [11], the building presents a rocking collapse mechanism of the BC façade, mainly due to the absence of interlocking with its perpendicular walls. Of course, this implies a very low resistance to seismic actions and a restoration intervention is proposed in [11] in order to improve interlocking between perpendicular walls and floors stiffness, so aiming at a global failure mechanism.

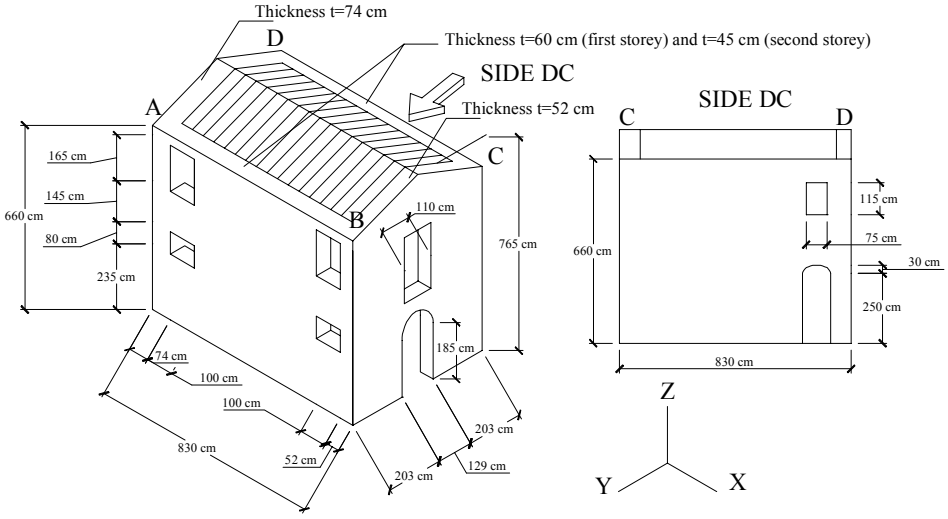

Figure 8: Ancient masonry house case study, geometry.

In the simulation here presented, only the building after the restoration intervention proposed in [11] is taken into consideration. The intervention provides a new wooden beam floor at the first floor, as well as the installation of steel tie elements at floor level. Furthermore, the roof structures are strengthened in order to provide in-plane load distribution capacity. The construction of a concrete element at the top of the walls with an embedded steel bar have been also proposed.

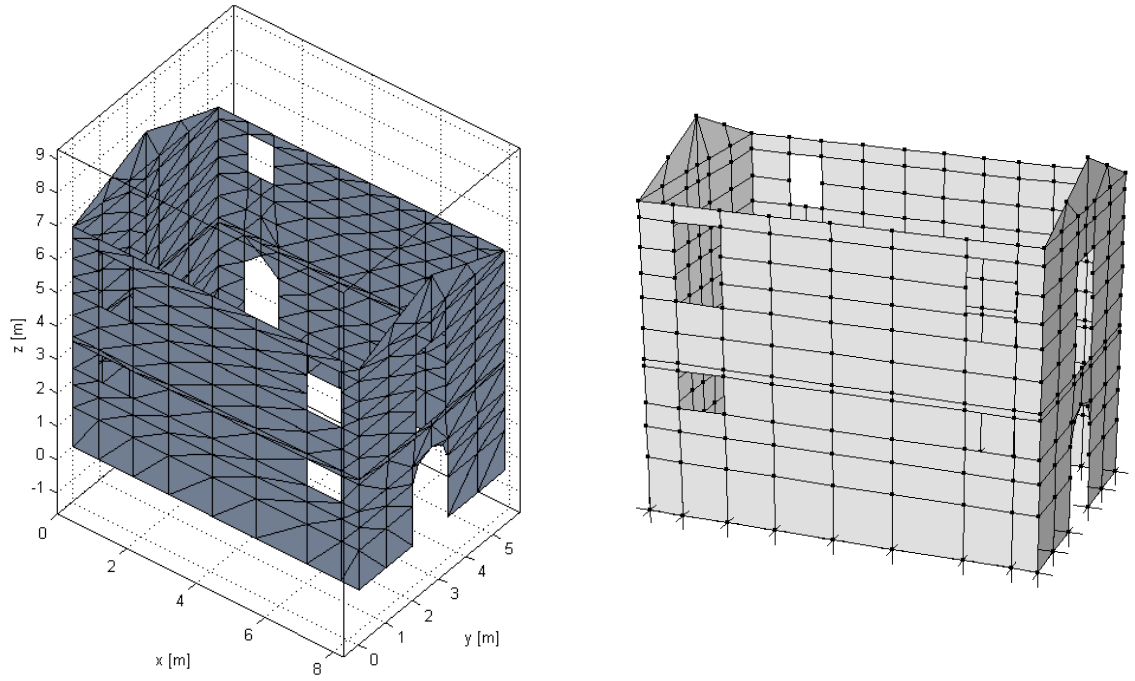

-a -b

Figure 9: -a: Mesh used for the limit analysis (1576 triangular elements) and (-b) mesh used in Strand 7 for an elastic-plastic analysis with Mohr-Coulomb failure criterion.

Masonry after the restoration intervention is constituted by bocks of dimensions 46x14x22 cm. In the homogenized FE limit analysis model, for joints reduced to interfaces a pure Mohr-Coulomb failure criterion with friction angle $\Phi = 30°$ and cohesion $c = 0.01 N/mm^2$ is adopted, in order to represent the very low tensile strength of masonry, whereas blocks are supposed infinitely resistant.

In the 3D FE limit analysis model, a mesh with 636 triangular elements is used, as shown in Figure 9-a.

The results obtained with the homogenized FE limit analysis model (i.e. failure shear at the base and failure mechanism) are compared with a standard FE elastic-perfectly plastic analysis performed by means of a commercial code, Figure 9-b. The analysis is conducted using a mesh of 324 four noded plate elements supposing masonry isotropic with a pure Mohr-Coulomb failure criterion ($c = 0.01 N/mm^2$ and $\Phi = 30°$).

The kinematic FE homogenized limit analysis gives a total shear at the base of the building of $701 kN$, in excellent agreement with the results obtained with the standard FE procedure ($710 kN$). In Figure 10-a total shear at the base obtained by means of the FE commercial code against node N displacement (see Figure 10-b) is reported. Furthermore, a comparison between deformed shapes at collapse of both models, Figure 10-b and Figure 11, shows the accuracy of the homogenized model and that failure is mainly concentrated on wall BC.

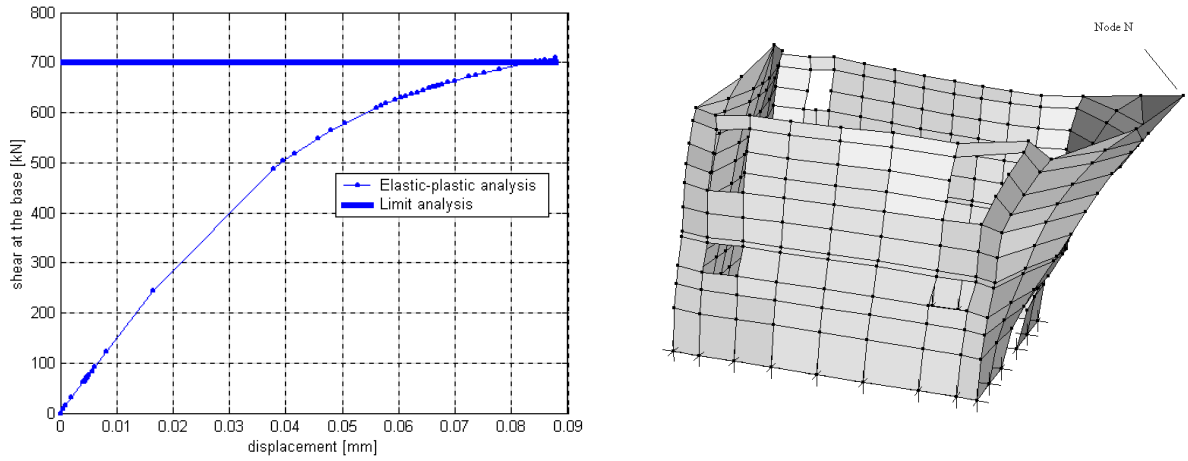

-a -b

Figure 10: Via Arizzi house, standard FE elastic plastic approach. Shear at the base - node N displacement curve. -b: deformed shape at collapse.

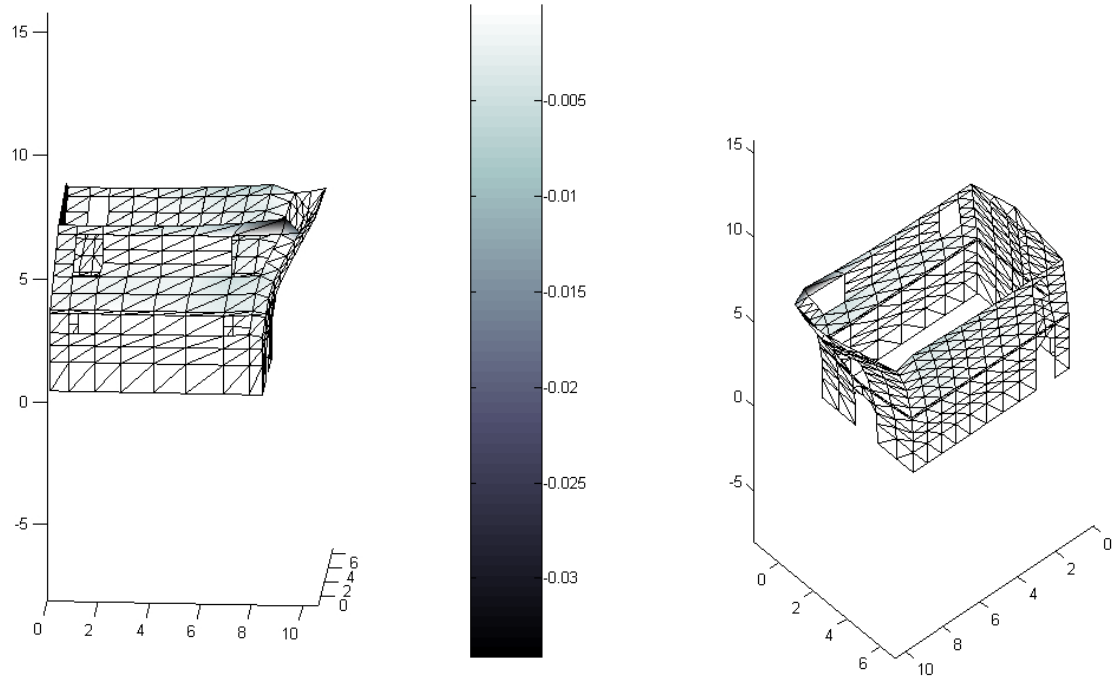

Figure 11: Deformed shape at collapse and concentration of plastic dissipation for the entire building, homogenization FE limit analysis approach.

Finally it is worth noting that the proportionality coefficient (defined as the ratio between horizontal load at failure and vertical loads) obtained with the homogenization model at hand is approximately equal to 0.36, in good agreement with that found in [17] (0.38).

5 CONCLUSIONS

In the present paper a kinematic FE limit analysis approach for the 3D analysis of masonry buildings subjected to horizontal actions has been presented. Both in- and out-of-plane failures are taken into account in the evaluation of the total internal power dissipated.

Meaningful examples have been treated with the model at hand and comparisons with standard incremental elastic-plastic procedures have been reported, in order to test the reliability of the homogenized model developed in terms of both collapse mechanism and ultimate shear at the base.

ACKNOWLEDGMENTS

A.Tralli and G.Milani gratefully acknowledge the support of the research project MIUR COFIN 2005 – Resistenza e degrado di interfacce in materiali e sistemi strutturali. Coordinator: Prof. A. Corigliano.

A.Tralli and G.Milani gratefully acknowledge Ing. G.Andrighetti (Head Engineer) and Ing. G.Galvan of the "Provincia di Ferrara".

REFERENCES

[1] L. Ramos, P.B. Lourenço, Modeling and vulnerability of historical city centers in seismic areas: a case study in Lisbon. *Engineering Structures*, **26**, 1295-1310, 2004.

[2] A. Giuffrè (editor), *Safety and conservation of historical centers: the Ortigia case*. Editore Laterza, Roma - Bari, 1993 [in Italian].

[3] G. Milani, P.B. Lourenço, A. Tralli, Homogenised limit analysis of masonry walls. Part I: failure surfaces. *Comp. Struct.*, **84**, 166-180, 2006.

[4] G. Milani, P.B. Lourenço, A. Tralli, A homogenization approach for the limit analysis of out-of-plane loaded masonry walls. Accepted for publication in *ASCE Journal of Structural Engineering*, 2006.

[5] O.P.C.M. 3274, 20/03/2003, Primi elementi in materia di criteri generali per la classificazione sismica del territorio nazionale e di normative tecniche per le costruzioni in zona sismica [in Italian].

[6] O.P.C.M. 3431/05 09/05/2005, Ulteriori modifiche ed integrazioni all'OPCM 3274/03 [in Italian].

[7] P.B. Lourenço, R. de Borst, J.G. Rots, A plane stress softening plasticity model for orthotropic materials. *International Journal for Numerical Methods in Engineering*, **40**, 4033-4057, 1997.

[8] A. Zucchini, P.B. Lourenço, A micro-mechanical model for the homogenisation of masonry. *International Journal of Solids and Structures*, **39**, 3233-3255, 2002.

[9] P. Suquet, Analyse limite et homogeneisation. *Comptes Rendus de l'Academie des Sciences - Series IIB – Mechanics*, **296**, 1355-1358, 1983.

[10] G. Milani, P.B. Lourenço, A. Tralli, Homogenised limit analysis of masonry walls. Part II: structural examples. *Comp. Struct.*, **84**, 181-195, 2006.

[11] R. De Benedictis, G. de Felice, A. Giuffrè, *Safety and Conservation of Historical Centres: The Ortigia Case, Chapter 9 Seismic Retrofit of a Building*. 189–217. A. Giuffrè, Editori Laterza, 1991.

[12] S.W. Sloan, P.W. Kleeman, Upper bound limit analysis using discontinuous velocity fields. *Computer Methods in Applied Mechanics and Engineering*, **127 (1-4)**, 293-314, 1995.

[13] J. Munro, A.M.A. Da Fonseca, Yield-line method by finite elements and linear programming. *J. Struct. Eng. ASCE*, **56B**, 37-44, 1978.

[14] A.A. Cannarozzi, M. Capurso, F. Laudiero, An iterative procedure for collapse analysis of reinforced concrete plates. *Computer Methods in Applied Mechanics and Engineering*, **16**, 47-68, 1978.

[15] S.W. Sloan, A steepest edge active set algorithm for solving sparse linear programming problems. *International Journal Numerical Methods Engineering*, **12**, 61-67, 1988.

[16] P.C. Olsen, Rigid-plastic finite element analysis of steel plates, structural girders and connections. *Computer Methods in Applied Mechanics and Engineering*, **191**, 761-781, 2001.

[17] A. Orduna, *Seismic assessment of ancient masonry structures by rigid blocks limit analysis*. PhD Thesis 2003. University of Minho, Portugal. Available at www.civil.uminho.pt/masonry.

[18] P.B. Lourenço, *Computational strategies for masonry structures.* PhD Thesis 1996. Delft University of Technology, the Netherlands. Available at www.civil.uminho.pt/masonry.

[19] P.B. Lourenço, J. Rots, A multi-surface interface model for the analysis of masonry structures. *Journal of Engineering Mechanics ASCE*, **123 (7)**, 660-668, 1997.

[20] D.M. 16/01/1996 (G.U. 5-2-1996, N. 29), Norme tecniche relative ai "Criteri generali per la verifica di sicurezza delle costruzioni, e dei carichi e sovraccarichi" [in Italian].

[21] A. Brencich, L. Gambarotta, S. Lagomarsino, *Catania Project: Research on the seismic response of two masonry buildings. Chapter 6: Analysis of a masonry building in Via Martoglio.* University of Genoa. CNR Gruppo Nazionale per la Difesa dei Terremoti, 107-151, 2000 [in Italian].

[22] G. Magenes, C. Braggio, *Catania Project: Research on the seismic response of two masonry buildings. Chapter 7: Analysis of a masonry building in Via Martoglio*. University of Pavia (in Italian). CNR Gruppo Nazionale per la Difesa dei Terremoti, 153-190, 2000.